constants, we have

$$\frac{\partial \hat{Y}_n}{\partial \hat{y}_n} = \frac{\partial \hat{\Gamma}\hat{y}_n}{\partial \hat{y}_n} = \hat{\Gamma}\frac{\partial \hat{y}_n}{\partial \hat{y}_n} = \hat{\Gamma}\boldsymbol{I} = \hat{\Gamma} \tag{14}$$

where $\boldsymbol{I}$ is the identity matrix. Similarly

$$\frac{\partial \hat{x}_n}{\partial \hat{X}_n} = \hat{\Gamma}^{-1}. \tag{15}$$

If we define $\hat{\beta}_n = [\beta_{pm}]_n = \hat{g}_n\hat{\Gamma}^{-1}$, the operation $\hat{\Gamma}\hat{\beta}_n$ in (13) is nothing more than the Fourier transform of $\hat{\beta}_n$ and the NFFT can be used to efficiently accomplish the transform. We note that a single column, $\hat{\beta}_{m,n}$, of the two-dimensional matrix $\hat{\beta}_n$ is of the same size as the data vector $\hat{y}_n$. So the premultiplication of $\hat{\beta}_{m,n}$ by $\hat{\Gamma}$ in (13) corresponds exactly to the operation in (3), and the same transform and data structure used for the circuit variables can be used in determining the frequency-domain derivatives. Thus (13) is accomplished for the mth frequency of $\boldsymbol{X}_n$ by use of the transform operator

$$\frac{\partial \boldsymbol{Y}_n}{\partial X_{m,n}} = \left[\frac{\partial Y_p}{\partial X}\right]_n = \mathcal{F}(\beta_m)_n \tag{16}$$

where $\partial \boldsymbol{Y}_n/\partial X_{m,n}$ is an N-dimensional matrix from which the elements of the Jacobian can be extracted. Again, the matrix $\beta_{m,n}$ (and thus $\partial \boldsymbol{Y}_n/\partial X_{m,n}$) is the same size as the data matrices $\boldsymbol{x}_n$, $\boldsymbol{X}_n$, $\boldsymbol{y}_n$, and $\boldsymbol{Y}_n$.

When Newton's method is accomplished using strictly real quantities, the following four quantities must be computed:

$$^{RR}j_{m,n} = \frac{\partial \operatorname{Re}(Y_n)}{\partial \operatorname{Re}(X_{m,n})} \tag{17}$$

$$^{RI}j_{m,n} = \frac{\partial \operatorname{Re}(Y_n)}{\partial \operatorname{Im}(X_{m,n})} \tag{18}$$

$$^{IR}j_{m,n} = \frac{\partial \operatorname{Im}(Y_n)}{\partial \operatorname{Re}(X_{m,n})} \tag{19}$$

$$^{II}j_{m,n} = \frac{\partial \operatorname{Im}(Y_n)}{\partial \operatorname{Im}(X_{m,n})} \tag{20}$$

but the procedure (16) produces the quantity

$$\mathcal{F}(\beta_{m,n}) = {}^{RR}j_{m,n} + {}^{II}j_{m,n} + j\left({}^{RI}j_{m,n} + {}^{IR}j_{m,n}\right) \tag{21}$$

and the individual components cannot be recovered. We form ${}^{R}\beta_{m,n} = \operatorname{Re}(\beta_{m,n})$ and ${}^{I}\beta_{m,n} = \operatorname{Im}(\beta_{m,n})$ as

$${}^{R}\beta_{m,n} = g_n \operatorname{Re}\left(\Gamma_m^{-1}\right) \tag{22}$$

and

$${}^{I}\beta_{m,n} = g_n \operatorname{Im}\left(\Gamma_m^{-1}\right). \tag{23}$$

Then following (16) we get

$$\mathcal{F}\left({}^{R}\beta_{m,n}\right) = {}^{RR}j_{m,n} + j\,{}^{IR}j_{m,n} \tag{24}$$

$$\mathcal{F}\left({}^{I}\beta_{m,n}\right) = {}^{RI}j_{m,n} + j\,{}^{II}j_{m,n} \tag{25}$$

from which the needed derivatives are available.

V. Discussion and Conclusion

Equations (24) and (25) can be efficiently implemented in a circuit simulator since no matrix multiplications are required. The operations in (22) and (23) are *scalar* multiplications. This results from the fact that the nonlinear constitutive relations are algebraic ($\hat{g}_n = \partial \hat{y}_n/\partial \hat{x}_n$ is a diagonal two-dimensional matrix). The γ_{km}^{-1} are constants and need be computed only once per simulation. However, the values of g_n are dependent on the nonlinear constitutive relations and so they change from iteration to iteration. For each iteration they are computed once and are then used in determining all the $\beta_{m,n}$ in β_n. The major operation is the multidimensional Fourier transform, which is performed once at each frequency of $\boldsymbol{X}_n$.

The method presented for evaluating the Jacobian permits the use of the efficient NFFT algorithm in conjunction with Newton's method for the harmonic balance analysis of nonlinear analog circuits. This procedure has been implemented in FREDA, a general nonlinear circuit simulator. The MESFET amplifier circuit of Chang *et al.* [4] was driven by two incommensurate input signals, one at 0 dBm and the other at 5 dBm, and simulated using 14 analysis frequencies. The time-domain element response was oversampled [5] so that the transform contained 26 frequencies. The solution was obtained in 1.1 s after 11 iterations using a modified Sămanskii method on a DEC DS 3100 workstation. The equivalent simulation using a matrix multiplication based transform (APDFT) required 3.8 s.

References

[1] A. Ushida and L. O. Chua, "Frequency-domain analysis of nonlinear circuits driven by multi-tone signals," *IEEE Trans. Circuits Syst.*, vol. CAS-31, pp. 766–779, Sept. 1984.

[2] K. S. Kundert, G. B. Sorkin, and A. Sangiovanni-Vincentelli, "Applying harmonic balance to almost-periodic circuits," *IEEE Trans. Microwave Theory Tech.*, vol. 36, pp. 366–377, Feb. 1988.

[3] V. Rizzoli, C. Cecchetti, A. Lipparini, and F. Mastri, "General-purpose harmonic balance analysis of nonlinear microwave circuits under multitone excitation," *IEEE Trans. Microwave Theory Tech.*, vol. 36, pp. 1650–1660, Dec. 1988.

[4] C. R. Chang, M. B. Steer, and G. W. Rhyne, "Frequency domain spectral balance using the arithmetic operator method," *IEEE Trans. Microwave Theory Tech.*, vol. 37, pp. 1681–1688, Nov. 1989.

[5] P. L. Heron, C. R. Chang, and M. B. Steer, "Control of aliasing in the harmonic balance simulation of nonlinear microwave circuits," in *IEEE MTT-S Int. Microwave Symp. Dig.*, June 1989, pp. 355–358.

Harmonic Balance and Frequency-Domain Simulation of Nonlinear Microwave Circuits Using the Block Newton Method

CHAO-REN CHANG, PATRICK L. HERON, AND MICHAEL B. STEER, MEMBER, IEEE

***Abstract*—An efficient algorithm using block Newton and chord methods is presented for the iterative minimization of the spectral balance error in the analysis of nonlinear microwave circuits. This algorithm is used in the harmonic balance and frequency-domain spectral balance simulation of a MESFET amplifier with single-tone and two-tone excitation.**

I. Introduction

Methods of nonlinear microwave analog circuit analysis can be classified by the nature of the linear and nonlinear subcircuit calculations: time-domain methods, where all elements are ana-

Manuscript received April 10, 1989; revised December 11, 1989. This work was supported by a National Science Foundation Presidential Young Investigator Award (Grant ECS-8657836) to M. B. Steer, by a grant from the Digital Equipment Corporation, and by an MTT graduate fellowship to P. L. Heron.

The authors are with the Electrical and Computer Engineering Department, North Carolina State University, Raleigh, NC 27695-7911.

IEEE Log Number 8934025.

0018-9480/90/0400-0431$01.00 ©1990 IEEE

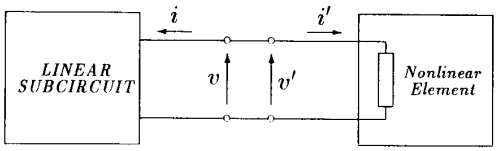

Fig. 1. A network partitioned into a linear subcircuit and a nonlinear element.

lyzed in the time domain; frequency-domain methods, where all elements are analyzed in the frequency domain; and hybrid methods, including the harmonic balance methods, which combine time-domain and frequency-domain analyses.

Most time-domain nonlinear circuit simulation methods are not suited to microwave applications [1]. Consequently the harmonic balance (HB) technique, which interfaces the frequency-domain analysis of the linear part of a circuit with the conventional time-domain analysis of the nonlinear part of a circuit, is increasingly being used. A significant amount of research in this field has been published [2]–[10], and the HB method is becoming a preferred nonlinear microwave circuit CAD technique. However, one of the disadvantages of HB methods is the aliasing problem [11]. Because of the errors introduced by aliasing, oversampling in the Fourier transform and inverse Fourier transform operations is often used in HB methods at the cost of increased run time.

Alternative techniques using a frequency-domain spectral balance method (FDSB) are based on power-series descriptions of nonlinear elements [12]–[17]. Without explicit time-domain calculations, FDSB methods avoid the aliasing problem and can often obtain higher accuracies than HB methods for the same set of analysis frequencies. However, the necessity of having a power-series description of the nonlinear elements instead of an arbitrary current–voltage relationship is the major disadvantage of most FDSB methods.

The purpose of the work reported here is to introduce a minimization algorithm which combines a block Newton iteration scheme with the Shamanskii method [12], [18] and then to present numerical results for HB and FDSB analyses using this technique. Comparisons of memory use and computer time are presented in detail. In particular, we consider the almost periodic discrete Fourier transform (APDFT) HB method [4], [9] with the dual frequency set (oversampling) algorithm [11] and the generalized power-series analysis using the arithmetic operator method (GPSA–AOM) [12]—an FDSB technique. A MESFET model [12] in which the nonlinear elements have power-series descriptions is used, since it can be simulated with both HB and GPSA–AOM.

II. Analysis of the Nonlinear System

The basic approach used to solve a system of nonlinear circuit equations is first to formulate an error function and then to use function-minimization algorithms such as the Newton iteration scheme. The classical approach to formulating the error function is to partition the circuit into linear and nonlinear subcircuits and, following separate analyses of the subcircuits, determine the steady state "balance" point of the system. For example, in Fig. 1, i, v and i', v' are the current and voltage of the linear subcircuit and the nonlinear element, respectively. With I_k, V_k and I_k', V_k' representing the phasor forms of i, v and i', v' at a particular radian frequency ω_k, and with $K+1$ different frequency components, the current at ω_k in a nonlinear admittance is a function of all voltage components V_k' $(k=-K,\cdots,0,\cdots,K)$ across the element:

$$I_k' = f(V_{-K}', \cdots, V_0', \cdots, V_K'), \qquad V_k = V_k'. \tag{1}$$

The voltage of ω_k in a nonlinear impedance is a function of all current components I_k' $(k=-K,\cdots,0,\cdots,K)$ in the element:

$$V_k' = g(I_{-K}', \cdots, I_0', \cdots, I_K'), \qquad I_k = -I_k'. \tag{2}$$

The difference between the hybrid methods and the frequency-domain methods is that the functions $f(x)$ and $g(x)$ are determined in the time domain or in the frequency domain, respectively.

To handle both impedance and admittance nonlinearities, both of Kirchhoff's laws must be satisfied. That is, the zero of the objective function

$$E = \sum_{k=0}^{K} |I_k + I_k'|^2 + \sum_{k=0}^{K} |V_k - V_k'|^2$$

must be found. In general, if we have L different nodes between the two subcircuits and M different nonlinear impedance type elements in the nonlinear subcircuit, the system objective will be

$$E = \sum_{k=0}^{K} \left(\sum_{p=1}^{L} |I_{p,k} + I_{p,k}'|^2 + \sum_{q=1}^{M} |V_{q,k} - V_{q,k}'|^2 \right).$$

Although it can be time consuming, the Newton method is frequently used in nonlinear circuit analysis to minimize E.

Let $\boldsymbol{x}$ represent the variable vector which is composed of all the required real and imaginary parts of the phasors of the node voltages and branch currents at $K+1$ different frequencies; variable $\boldsymbol{x}_k$ represents the component of $\boldsymbol{x}$ at frequency ω_k; vector $\boldsymbol{f}(\boldsymbol{x})$ represents the error function and is composed of all the corresponding $I_{j,p,k} + I_{j,p,k}'$ and $V_{j,q,k} - V_{j,q,k}'$; and $\boldsymbol{f}_k(\boldsymbol{x})$ represents the component of $\boldsymbol{f}(\boldsymbol{x})$ having frequency ω_k. In the Newton method, the objective function E is minimized with respect to $\boldsymbol{x}$ using the iterative procedure

$${}^{i+1}\boldsymbol{x} = {}^{i}\boldsymbol{x} - \boldsymbol{J}^{-1}({}^{i}\boldsymbol{x})\, \boldsymbol{f}({}^{i}\boldsymbol{x}) \tag{3}$$

where the leading superscripts are iteration numbers and the matrix $\boldsymbol{J}$ is the Jacobian matrix. For increased program efficiency, a modified Newton method [19] (block Newton method) can also be used. That is, $K+1$ separate iterative procedures

$${}^{i+1}\boldsymbol{x}_k = {}^{i}\boldsymbol{x}_k - \boldsymbol{J}_k^{-1}({}^{i}\boldsymbol{x})\, \boldsymbol{f}_k({}^{i}\boldsymbol{x}), \qquad k=0,1,\cdots,K \tag{4}$$

can be solved simultaneously. In this case, the matrix inverse calculation time is approximately $(K+1)^{\alpha}$ times faster than the time needed in the full Jacobian form of the Newton method, where the typical value of α is generally between 0.5 and 2 and is determined by the matrix inversion algorithm [20]. Further increases in efficiency can be obtained by using the chord method which uses the previously computed $\boldsymbol{J}^{-1}$ (or $\boldsymbol{J}_k^{-1}$) for the present iteration regardless of the method used in the previous iteration.

III. Comparisons and Discussion

The device used for the comparisons is the medium-power GaAs MESFET (Avantek AT8250) which was previously used in [12], where the equivalent circuit and parameter values are given.

One property we compare here is the accuracy of each simulation method as a function of the number of frequency components considered. The first example is the class-A MESFET amplifier with a 10 dBm single-tone input (this corresponds to 3.6 dB gain compression) at 3 GHz. Fig. 2 shows the simulated output power at the second-harmonic frequency, in which curve a is for the GPSA–AOM and curve b is for the APDFT HB method. Curves a and b in Fig. 2 show a significant difference between these two techniques. The simulated result of curve b, for the APDFT HB method, is not stable until the number of analysis frequencies is 15.

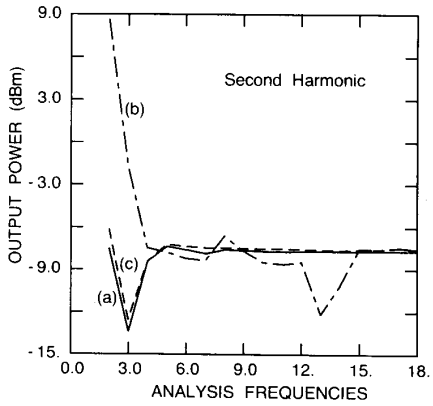

Fig. 2. Comparison of the simulated output power versus the number of analysis frequencies at the second harmonic frequency for the MESFET amplifier with single-tone input excitation. *a*: GPSA–AOM; *b*: APDFT HB method; *c*: dual-frequency-set APDFT HB method.

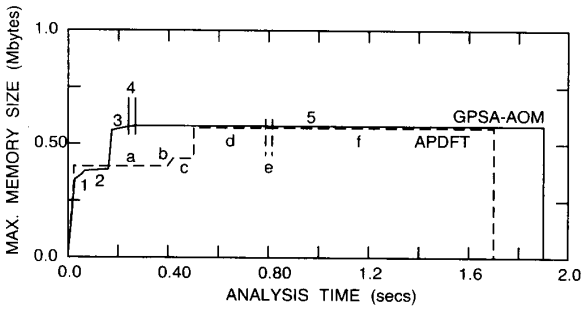

Fig. 3. Comparison of simulation run time and the maximum memory requirement for the MESFET amplifier with single-tone input excitation. The solid line is for the GPSA–AOM and the dashed line is for the dual-frequency-set APDFT HB method. The regions designated are listed in Table I. Computer run time is for a DEC DS3100 workstation.

TABLE I
THE PROCESSES EXECUTED IN EACH TIME SEGMENT OF FIGS. 3 AND 5

Region		Processes
GPSA-AOM	APDFT	
—	*a*	Set up the transform matrix
1	*b*	Initialize the DC variables
2	*c*	Linear subcircuit calculations including matrix formulations and reductions
3	*d*	block Newton method including system error and gradient calculations
4	*e*	Jacobian inversions
5	*f*	Iterations with chord method including system error evaluations (31 cycles for single-tone test, 6 cycles for two-tone test)

The APDFT HB method involves the forward and backward Fourier transforms to convert the signals between time- and frequency-domain representations. Insufficient sampling of the signals in either the time or the frequency domain introduces aliasing. Because the sampling rate is directly related to the number of frequencies considered in the analysis, a larger number of analysis frequencies yields greater accuracy for the APDFT technique. This is not only because of reduced aliasing effects, but also because the broader spectrum better represents the signal. With GPSA–AOM, a larger frequency spectrum also better represents circuit voltages and currents. With both techniques, simulation with fewer frequencies generally results in higher errors but the growth in error for the APDFT HB method is greater than that for GPSA–AOM.

In order to incorporate a sufficient number of frequencies to avoid aliasing during the Fourier transforms and also to decrease the number of frequencies in the frequency-domain calculations, the dual frequency set algorithm (oversampling in the nonlinear analysis) for harmonic balance methods [11] was used. Curve *c* in Fig. 2 shows the simulated result using the APDFT, where the number of frequencies in the Fourier transforms is kept at 15. If we assume that the acceptable maximum error limit is 0.1 dB, then from curves *a* and *c* in Fig. 2 the GPSA-AOM requires eight analysis frequencies to converge the output power level of the second harmonic to the acceptable limit whereas the improved APDFT method requires seven frequencies.

A more detailed comparison of the computer run times and memory requirements for this example is made in Fig. 3 under the following conditions: eight analysis frequencies are used in the GPSA–AOM and seven analysis frequencies with 15 transform frequencies in the dual frequency set APDFT HB method. In Fig. 3, the solid line is for the GPSA–AOM and the dashed line is for the dual frequency set APDFT HB method. The simulations were performed on a DEC DS3100 workstation (rated at 13 VAX 11/780 MIPS). The process executed in each time segment in Fig. 3 is listed in Table I. In this example, both techniques have similar computer run time and memory requirement to achieve the same accuracy. Both techniques consume most of their CPU time in the nonlinear analyses; only a small part (less than 0.1 s) is required to formulate and to reduce the modified nodal admittance matrices of the linear subcircuit. Both methods took one block Newton iteration and 31 chord iterations to converge the system error to the specified limit. The full-Jacobian Newton method is not required in this case and the time required for the inversion of the block Jacobian matrix is insignificant.

The second example is an analysis of the same amplifier having two-tone excitation [12]. One ac source is the local oscillator (LO) at 2.4 GHz and 0 dBm input power. The other source is the RF signal at 2.35 GHz and −10 dBm input power. The 50 MHz IF signal is detected. Fig. 4 shows the simulated IF output power as a function of the intermodulation order. As before, there is aliasing error and the conventional APDFT HB method converges to the correct result at the fifth intermodulation order (see curve *b*). Again the dual-frequency-set algorithm improves this situation. With fifth-order intermodulation in the Fourier transforms and various intermodulation orders in the frequency-domain analysis, the simulated results of the dual-frequency-set APDFT HB methods are shown as curve *c*. Fig. 5 presents detailed comparisons between these two techniques using analysis frequencies corresponding to second-order intermodulation (six ac and one dc). Frequencies corresponding to fifth-order intermodulation (30 ac and one dc) were used for the Fourier transforms in the APDFT. The process executed in each time segment is listed in Table I. In this case the GPSA–AOM is more efficient than the dual-frequency-set APDFT HB method. Since the intermodulation order for the transform frequencies is set at 5, the dual-frequency-set APDFT HB method spends much of its time in the transform matrix formulation, system-error evaluations, and the gradient calculation. The nonlinear analysis in the GPSA–AOM is about ten times faster than the dual-frequency-set APDFT HB method in this example. These results are typical of those we have obtained with other two-tone excitation problems.

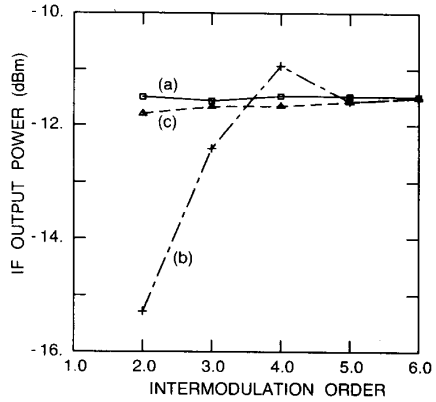

Fig. 4. Comparison of the simulated IF (50 MHz) output power versus the intermodulation order for the MESFET amplifier with two-tone input excitation. *a*: GPSA–AOM; *b*: APDFT HB method; *c*: dual-frequency-set APDFT HB method.

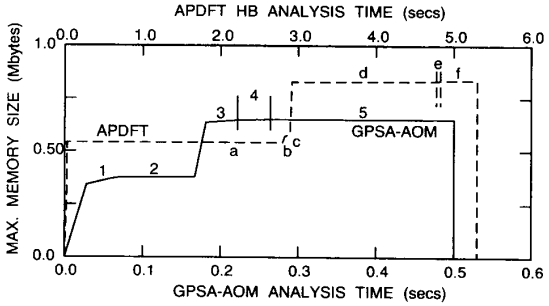

Fig. 5. Comparison of simulation run time and the maximum memory requirement for the MESFET amplifier with two-tone input excitation. The solid line is for the GPSA–AOM and the dashed line is for the dual-frequency-set APDFT HB method. The regions designated are listed in Table I. Computer run time is for a DEC DS3100 workstation.

IV. Conclusion

This paper presented a common error minimization algorithm for performing both the harmonic balance and the frequency-domain spectral balance analysis of nonlinear analog circuits. Simulations of a MESFET amplifier having one- and two-tone excitations were used to compare the performances of the GPSA–AOM and APDFT harmonic balance techniques. In general, based on the same accuracy consideration, the performance of the APDFT harmonic balance method is comparable to the GPSA–AOM with single-tone input excitation. The GPSA–AOM tends to dominate in circuits with two or more incommensurable signals. However, from the device-modeling viewpoint, most FDSB methods are limited to power-series-based models and thus have less utility than harmonic balance methods which use nonlinear models described by arbitrary functional relations.

References

[1] V. Rizzoli and A. Neri, "State of the art and presented trends in nonlinear microwave CAD techniques," *IEEE Trans. Microwave Theory Tech.*, vol. 36, pp. 343–365, Feb. 1988.

[2] M. S. Nakhla and J. Vlach, "A piecewise harmonic-balance technique for determination of periodic response of nonlinear systems," *IEEE Trans. Circuits Syst.*, vol. CAS-23, pp. 85–91, Feb. 1976.

[3] L. O. Chua and A. Ushida, "Algorithms for computing almost periodic steady-state response of nonlinear systems to multiple input frequencies," *IEEE Trans. Circuits Syst.*, vol. CAS-28, pp. 953–971, Oct. 1981.

[4] A. Ushida and L. O. Chua, "Frequency-domain analysis of nonlinear circuits driven by multi-tone signals," *IEEE Trans. Circuits Syst.*, vol. CAS-31, pp. 766–779, Sept. 1984.

[5] K. S. Kundert and A. Sangiovanni-Vincentelli, "Simulation of nonlinear circuits in the frequency domain," *IEEE Trans. Computer-Aided Design*, vol. CAD-5, pp. 521–535, Oct. 1986.

[6] R. Gilmore, "Nonlinear circuit design using the modified harmonic balance algorithm," *IEEE Trans. Microwave Theory Tech.*, vol. MTT-34, pp.1294–1307, Dec. 1986.

[7] V. Rizzoli, C. Cecchetti, and A. Lipparini, "A general-purpose program for the analysis of nonlinear microwave circuits under multitone excitation by multidimensional Fourier transform," in *Proc. 17th European Microwave Conf.*, 1987, pp. 635–640.

[8] C. Camacho-Penalosa, "Numerical technique for determining steady-state response of nonlinear circuits to multitone input signals," *Electron. Lett.*, vol. 23, pp. 828–829, July 1987.

[9] K. S. Kundert, G. B. Sorkin, and A. Sangiovanni-Vincentelli, "Applying harmonic balance to almost-periodic circuits," *IEEE Trans. Microwave Theory Tech.*, vol. 36, pp. 366–377, Feb. 1988.

[10] V. Rizzoli, C. Cecchetti, A. Lipparini, and F. Mastri, "General-purpose harmonic balance analysis of nonlinear microwave circuits under multitone excitation," *IEEE Trans. Microwave Theory Tech.*, vol. 36, pp. 1650–1660, Dec. 1988.

[11] P. L. Heron, C. R. Chang, and M. B. Steer, "Control of aliasing in the harmonic balance simulation of nonlinear microwave circuits," in 1989 *IEEE MTT-S Int. Microwave Symp. Dig.*, pp. 355–358.

[12] C. R. Chang, M. B. Steer, and G. W. Rhyne, "Frequency-domain spectral balance using the arithmetic operator method," *IEEE Trans. Microwave Theory Tech.*, vol. 37, pp. 1681–1688, Nov. 1989.

[13] M. Lamnabhi, "Functional analysis of nonlinear circuits: a generating power series approach," *Proc. Inst. Elec. Eng.*, vol 133, pp. 375–384, Oct. 1986.

[14] G. W. Rhyne and M. B. Steer, "Generalized power series analysis of intermodulation distortion in a MESFET amplifier: Simulation and experiment," *IEEE Trans. Microwave Theory Tech.*, vol. MTT-35, pp. 1248–1255, Dec. 1987.

[15] G. W. Rhyne, M. B. Steer, and B. D. Bates, "Frequency domain nonlinear circuit analysis using generalized power series," *IEEE Trans. Microwave Theory Tech.*, vol. 36, pp. 379–387, Feb. 1988.

[16] J. H. Haywood and Y. L. Chow, "Intermodulation distortion analysis using a frequency domain harmonic balance technique," *IEEE Trans. Microwave Theory Tech.*, vol. 36, pp. 1251–1257, Aug. 1988.

[17] S. Withington and E. L. Kollberg, "Spectral-domain analysis of harmonic effects in superconducting quasiparticle mixers," *IEEE Trans. Microwave Theory Tech.*, vol. 37, pp. 231–238, Jan. 1989.

[18] J. E. Dennis, Jr. and R. B. Schnabel, *Numerical Methods for Unconstrained Optimization and Nonlinear Equations*. Englewood Cliffs, NJ: Prentice-Hall, 1983.

[19] J. M. Ortega and W. C. Rheinboldt, *Iterative Solution of Nonlinear Equations in Several Variables*. New York: Academic Press, 1970.

[20] K. S. Kundert, "Sparse matrix techniques and their application to ciruit simulation," in A. E. Ruehli, *Circuit Analysis, Simulation and Design*, vol. 3, part 1. New York: North-Holland.

A New Resistance Measurement Technique Applicable to High-Temperature Superconducting Materials at Microwave Frequencies

MICHAEL K. SKREHOT AND KAI CHANG, SENIOR MEMBER, IEEE

***Abstract*—A two-gap electrically floating resonant strip is used for surface resistance measurements of the high-temperature superconductor $YBa_2Cu_3O_{7-\delta}$. The method used is simple, has no electrical contact, operates at various resonant frequencies, and requires only a small sample. An analysis was used that allows for the accurate design of the strip dimensions to produce a desired resonant frequency. Experimental measurements on resonant frequencies in *X*- and *Ku*-bands (8–18 GHz) agree well with the calculations. The method allows one to extract the normalized**

Manuscript received June 27, 1989; revised November 13, 1989. This work was supported in part by a Texas Instruments Fellowship and by the U.S. Army Research Office.

M. K. Skrehot was with the Department of Electrical Engineering, Texas A&M University, College Station, TX 77843. He is now with Texas Instruments, Inc., P.O. Box 655474, MS 255, Dallas, TX 75265.

K. Chang is with the Department of Electrical Engineering, Texas A&M University, College Station, TX 77843-3128.

IEEE Log Number 8934024.

0018-9480/90/0400-0434$01.00 ©1990 IEEE